Computational Technique for Compressible Vortex Flows Past Wings at Large Incidence

Osama A. Kandil*
Old Dominion University, Norfolk, Virginia

A computational technique based on the integral solution of the full potential equation has been developed for the solution of three-dimensional subcritical flows past wings at high angles of attack. The problem includes two sources of nonlinearities: a boundary-oriented nonlinearity (separated flow roll-up) and a region-oriented nonlinearity (flow compressibility). The former is represented by a nonlinear vortex lattice, while the latter is represented by a source distribution within a finite computational volume. The solution is obtained by using double iteration cycles, a separated flow (wake) iteration cycle, and a compressibility iteration cycle. The computational technique is applied to a delta wing and the results show that the technique is accurate, promising, and efficient.

Introduction

DEVELOPMENT of computational techniques for three-dimensional flows past wings at high angles of attack have become extremely important to aerodynamicists dealing with modern designs of fighter aircraft, missiles, and helicopters. Modern fighter aircraft fly at high angles of attack during takeoff, offensive and defensive maneuvering, approach, and landing. In this range of angle of attack, vortex flows develop around the aircraft that have dominant effects on its aerodynamic characteristics and controllability. Modern designs of missiles require high launch angles of attack and high maneuverability within which a very complex vortex flow develops. For helicopters, the interaction of a blade with the vortex wake of another blade affects its operating performance, vibration, and noise characteristics. In forward speeds, blade slap, a predominant source of external noise, occurs due to the rapid time rates of change of the pressure on the blade developing from the blade passage through a tip vortex of a preceding blade.

For all these applications, one has to deal with strong nonlinear aerodynamics. Compressibility and edge separation of the flow are the main sources of the strong nonlinear effects. Prediction of the aerodynamic characteristics under the coupled effects of nonlinearities is obviously a challenging problem because of the complexities involved in the flow.

An extensive literature review reveals that all of the existing techniques do not simultaneously and completely account for these two sources of nonlinearities. Some of the existing techniques can treat the problem with flow separation at sharp edges without accounting for the full nonlinear compressibility effects (limited to low Mach numbers), while the others can treat the problem with the full nonlinear compressibility without accounting for the roll-up of the separated flow (limited to small angles of attack).

Mathematically, a problem is called a nonlinear problem if the governing equation is nonlinear and/or if the boundary conditions are nonlinear. For inviscid, incompressible, or low-subsonic flows at high angles of attack, the problem is nonlinear, although the governing equation is linear (the Laplace or Prandtl-Glauert equation). The nonlinearity is due to the boundary conditions on the separated flow surfaces. On the other hand, for inviscid compressible flows at low angles of attack, the problem is nonlinear because the governing equation is nonlinear (full potential equation) even with linearized boundary conditions. For compressible flows at high angles of attack, the problem is obviously nonlinear due to both the governing equation and the boundary conditions.

In search for an appropriate numerical method of solution, one has to bear in mind the origin of nonlinearity: a boundary oriented (separated flow roll-up), a region oriented (flow compressibility), or both. For the boundary-oriented nonlinearity, methods that are directly or indirectly derived from the Green's function solution (integral equation methods) have been developed, such as the nonlinear discrete vortex,[1-6] doublet panel,[7-12] vortex panel,[13-15] and velocity potential panel,[16,17] among others. To account for the flow compressibility in these methods, the Prandtl-Glauert transformation based on the freestream Mach number is used. The computed results have shown that this transformation is limited to cases with low subsonic Mach numbers and high angles of attack or moderate-to-high subsonic Mach numbers and low angles of attack. For the region-oriented nonlinearity, finite difference methods have been extensively used[18-21] without addressing the roll-up of separated flow. However, for supersonic flows at high angles of attack, computationally expensive methods based on the full potential equation[22,23] and Euler's equations[24-26] have been developed. These methods use different versions of implicit and explicit finite difference techniques.

Recently, steady vortex flows about three-dimensional wings have been solved by using the time-marching finite volume techniques of the Euler equations. Rizzi[27] applied a pseudo unsteady explicit version of the technique to the steady transonic flow around wing/body configuration at angles of attack that did not exceed 3.06 deg. The convergence of the technique to steady flow has been accelerated by using a variable weighting factor and the local time-step technique. Tip vortex flow has been captured past the ONERA M6 wing by using a mesh of 18,000 cells and 310 s of CPU time on the Cyber 203 vector processor.

Krause et al.[28] also used a time-marching finite-volume technique for Euler and Navier-Stokes equations and applied it to the incompressible flow around a delta wing of aspect ratio of 1 and 15 deg angle of attack. In the Euler equations, numerical damping was necessary for the solution to converge and, in the Navier-Stokes equations, smooth flowfields were obtained only for Reynolds numbers of the order of a few

Presented as Paper 83-2078 at the AIAA Atmospheric Flight Mechanics Conference, Gatlinburg, TN, Aug. 15-17, 1983; received Nov. 1, 1983; revision received March 7, 1985.

*Professor, Department of Mechanical Engineering and Mechanics. Member AIAA.

hundred. It is apparent that their captured leading-edge vortex flow in the Euler equation solution is dependent upon the artificially introduced vorticity due to the damping nature of the technique. This had been confirmed earlier by Rizzi.[29] It is the author's opinion that a Kutta-like condition is needed for the uniqueness of Euler's equation solution. Alternatively, vortex sheet fitting can be used in conjunction with a modified time-marching technique of Euler's equation. Although the computations in Ref. 28 have been extended to 50% behind the trailing edge, the computed results did not show the formation of the trailing-edge vortex core that had been computed[5,6] and measured[31] earlier. Singular behavior of the finite difference technique at the wing leading edge has been reported and more future work is needed on this problem. The CPU time has not been reported in this work.

It is evident that integral equation methods are powerful and computationally economical in treating the boundary-oriented nonlinearity. Moreover, it has tentatively been demonstrated that they can treat the region-oriented nonlinearity in subcritical flows. This is achieved by treating the nonlinear compressible terms in the full potential equation as inhomogeneity and hence considering the result as a Poisson's equation. Thus, a volume integral term corresponding to the inhomogeneity is added to the surface integral terms in the expression of the field velocity, as will be shown later.

The integral equation (IE) approach has several advantages over the finite difference (FD) approach. The IE approach involves evaluation of integrals, which is more accurate and simpler than the FD approach in which the accuracy depends on the grid size. Moreover, the IE approach automatically satisfies the far-field boundary conditions and hence a small limited region around the source of disturbance is needed. In the FD approach, grid points are needed over a large region around the source of disturbance and special treatment is required to satisfy the far-field boundary conditions.

In this paper, a computational technique based on the IE approach has been developed and applied to a low-aspect-ratio delta wing at a large angle of attack in subcritical flows. Extension of this technique to transonic flows is underway.

Integral Equation Formulation

The three-dimensional, steady inviscid, compressible flow is governed by the following equations:

Conservation of mass

$$(\rho^*\Phi^*_{x^*})_{x^*} + (\rho^*\Phi^*_{y^*})_{y^*} + (\rho^*\Phi^*_{z^*})_{z^*} = 0 \tag{1}$$

Conservation of energy

$$a^{*2}_\infty + \frac{\gamma-1}{2}V^{*2}_\infty = a^{*2} + \frac{\gamma-1}{2}(\Phi^{*2}_{x^*} + \Phi^{*2}_{y^*} + \Phi^{*2}_{z^*}) \tag{2}$$

Isentropic gas equation

$$\rho^*/\rho_\infty = (a^{*2}/a^{*2}_\infty)^{1/(\gamma-1)} \tag{3}$$

where Φ^* is the total velocity potential, a^* the speed of sound, ρ^* the density, γ the ratio of specific heats, and subscript ∞ the freestream condition. Combining Eqs. (2) and (3) and using V^*_∞, ρ^*_∞, and a length ℓ as the reference parameters, we obtain the following dimensionless equation for the density ρ:

$$\rho = \left[1 + \frac{\gamma-1}{2}M^2_\infty(1-\Phi^2_x-\Phi^2_y-\Phi^2_z)\right]^{1/(\gamma-1)} \tag{4}$$

where M_∞ is the freestream Mach number.

The dimensionless form of Eq. (1) is given by

$$\Phi_{xx} + \Phi_{yy} + \Phi_{zz} = G \tag{5}$$

where

$$G = -(1/\rho)(\rho_x\Phi_x + \rho_y\Phi_y + \rho_z\Phi_z) \tag{6}$$

Reading Eq. (5) as Poisson's equation and using Green's theorem, the solution of the equation is given by the sum of surface and volume integral terms as well as the freestream velocity potential

$$\Phi_p(x,y,z) = \Phi_\infty + \frac{1}{4\pi}\oiint q\frac{1}{r}\,dS + \frac{1}{4\pi}\oiint \mu\frac{\partial}{\partial n}\left(\frac{1}{r}\right)dS + \frac{1}{4\pi}\iiint\frac{G}{r}\,dV \tag{7}$$

where $_p(x,y,z)$ is a field point, Φ_∞ the velocity potential of freestream, q the strength of a source distribution on the boundary, μ the strength of a doublet distribution on the boundary, G a source distribution throughout the flowfield representing the compressibility of the flow, and r given by

$$r = [(x-\xi)^2 + (y-\eta)^2 + (z-\zeta)^2]^{1/2} \tag{8}$$

It should be noted that Eq. (7) automatically satisfies the boundary condition at infinity. This is a big computational advantage over the finite difference technique, since one does not need to enforce this condition. Moreover, a small finite volume around the wing will be sufficient to solve the problem.

Taking the gradient of Eq. (7) and replacing the surface doublet term on the right-hand side by a surface vorticity term, we obtain the expression for the velocity field,

$$\bar V_p(x,y,z) = \bar e_\infty + \frac{1}{4\pi}\oiint\frac{q(\xi,\eta,\zeta)}{r^2}\bar e_r\,dS + \frac{1}{4\pi}\oiint\frac{\bar\omega(\xi,\eta,\zeta)x\bar r}{r^3}dS + \frac{1}{4\pi}\iiint\frac{G(\xi,\eta,\zeta)}{r^2}\bar e_r\,dV \tag{9}$$

For an incompressible flow, the volume integral term vanishes since $G=0$ and the resulting expression includes surface integral terms only. Moreover, if the wing is reduced to a lifting surface, the surface source term is not needed and the resulting expression represents the basic approach used in the nonlinear vortex lattice and the nonlinear vortex panel techniques developed earlier by the author.[2,14] In this case, the basic unknowns of the problem are the circulation distribution Γ (vortex lattice technique) or the vorticity distribution $\bar\omega$ (vortex panel technique), and the shape of the free vortex sheets emanating from the separation lines. These are obtained by imposing the no-penetration condition on the lifting surface, the Kutta condition along the separation edges, and the kinematic and dynamic boundary conditions on the free vortex sheets. This is accomplished by an iterative technique that will be modified later to include accurate modeling of the inviscid vortex cores.[5,6]

For low-to-moderate subsonic Mach numbers, the linearized compressibility effect is given by

$$G = M^2_\infty\Phi_{xx} \tag{10}$$

and on using this expression for G in Eq. (5), we recover the linear homogeneous equation

$$\beta^2\Phi_{xx} + \Phi_{yy} + \Phi_{zz} = 0 \tag{11}$$

where $\beta = (1-M^2_\infty)^{1/2}$. Following the Prandtl-Glauert transformation, the compressible flow of Eq. (11) is solved in the equivalent incompressible region.[30] In the compressible region, such a solution gives the first approximation of the strength G in Eq. (9).

For the full compressibility effects, the following iterative procedure is used. Starting with the approximate solution of G, Eq. (9) is used to calculate $\bar{V}_p$ and Eqs. (4) and (6) are used to update the values of G. Next, the boundary conditions are enforced iteratively, with G fixed, until we obtain the strengths of q and $\bar{\omega}$ (or q and Γ) and the shape of the free vortex sheets. Next, G is updated and the iteration cycles are repeated until the solution of $\bar{\omega}$, G, and the shape of the free vortex sheets converge.

Method of Solution and the Computational Technique

The method of solution is divided into two major steps. In the first step, linear compressibility effects are taken into account only through the Prandtl-Glauert transformation, while in the second, nonlinear compressibility effects are taken into account through Poisson's full potential flow equation. The details of these two major steps follow.

Step 1: Linear Compressibility Effects

1) Equation (11) is used to introduce the flow compressibility linearly. This is done by solving the problem in the equivalent incompressible region[30] governed by

$$\Phi_{x'x'} + \Phi_{y'y'} + \Phi_{z'z'} = 0 \tag{12}$$

where

$$x' = x/\beta,\ y' = y,\ z' = z,\ \beta = (1 - M_\infty^2)^{1/2} \tag{13}$$

Using the technique of Ref. 30 coupled with the modified nonlinear discrete vortex method of Ref. 6, we obtain the circulation distribution on the wing and its free vortex lines and the shape of the free vortex lines. It should be noted here that the shape of the free vortex lines is determined under the linear compressibility effects. Moreover, no volume integral terms have been used in this step.

2) Before switching to the nonlinear compressibility effects, a finite parallelopiped-shaped volume is taken around the wing and a three-dimensional grid is generated within this volume, see Fig. 1. Equation (10) is then used to calculate the linear G_i values (source strength) at the centroids of all the elemental volumes of the grid. In computing G_i values, Eq. (10) is rewritten as

$$G_i = M_\infty^2 u_{xi} \tag{14}$$

where u_{xi} is the sum of all x derivatives of the induced x component of velocity at the ith centroid due to all the vortex lines (bound and free) in the flowfield. Central finite differencing is used to calculate u_{xi} since the flow is assumed subcritical throughout. It should be noted that the G_i value is considered constant within the elemental volume ΔV_i.

A computer program is devoted for this step and the resulting solution (circulation distribution, coordinates of free vortex lines, and G_i distribution of the three-dimensional grid) is stored on a file.

Step 2: Nonlinear Compressibility Effects

This step includes a compressibility iteration cycle and a wake iteration cycle as follows:

1) Fixing the shape of the free vortex lines, Eqs. (4) and (6) are used to compute ρ_i and G_i as

$$\rho_i = \left[1 + \frac{\gamma - 1}{2} M_\infty^2 (1 - u_i^2 - v_i^2 - w_i^2)\right]^{1/(\gamma-1)} \tag{15}$$

$$G_i = -\frac{1}{\rho_i}(\rho_{xi} u_i + \rho_{yi} v_i + \rho_{zi} w_i) \tag{16}$$

where u_i, v_i, and w_i are the components of the freestream velocity and the ith induced velocity due to all the vortex lines and elemental source volumes [using Eqs. (A3-A5) of the Ap-

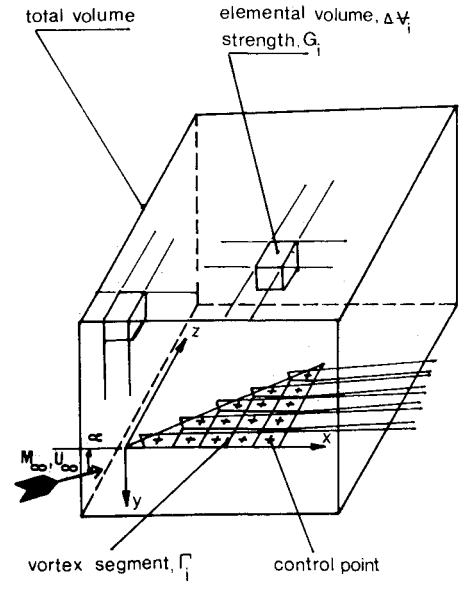

Fig. 1 Computational domain.

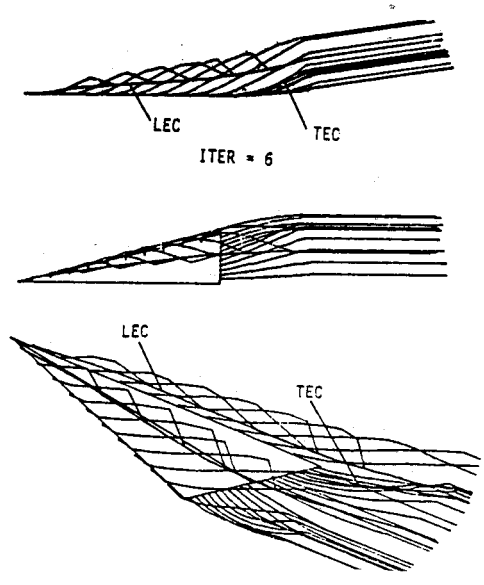

Fig. 2 Converged solution showing the computed vortex cores at $\mathcal{R} = 1$, $\alpha = 20.5$ deg, $M_\infty = 0.0$ ($G_i = 0.0$).

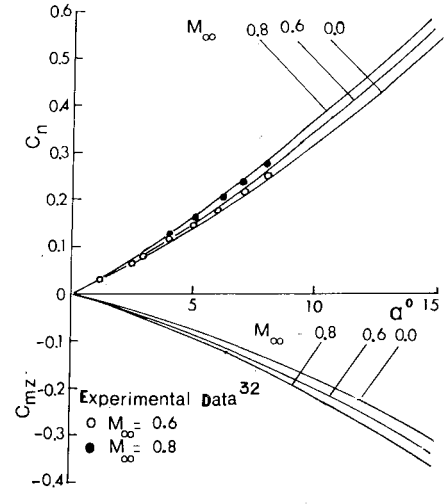

Fig. 3 Normal force and pitching moment coefficients vs angle of attack at different Mach numbers ($\mathcal{R} = 1.0$, $G_i = M_\infty u_{xi}$).

pendix]. Here, the density gradients ρ_{xi}, ρ_{yi}, and ρ_{zi} are also calculated using central finite differencing equations. This is the compressibility iteration cycle.

2) Fixing G_i values, the no-penetration condition is enforced on the wing, which is followed by enforcing the kinematic and dynamic boundary conditions on the free vortex lines. This is the wake iteration cycle. The compressibility and wake iteration cycles are successively repeated until the circulation and G_i distributions converge. The net surface pressure distribution is calculated by using the full compressible pressure coefficient equation

$$\Delta C_p = C_{p1} - C_{p2} = \frac{2}{\gamma M_\infty^2}\left\{\left[1+\frac{\gamma-1}{2}M_\infty^2(1-V_1^2)\right]^{\gamma/(\gamma-1)} - \left[1+\frac{\gamma-1}{2}M_\infty^2(1-V_2^2)\right]\right\}^{\gamma/(\gamma-1)} \tag{17}$$

where

$$\bar{V}_1 = \bar{e}_\infty + \bar{V}_G + \bar{V}_\Gamma + \bar{V}_{\Gamma S1}$$
$$\bar{V}_2 = \bar{e}_\infty + \bar{V}_G + \bar{V}_\Gamma + \bar{V}_{\Gamma S2} \tag{18}$$

where $\bar{V}_1$ and $\bar{V}_2$ are the total upper and lower velocity, $\bar{V}_G$ the induced velocity due to the source distribution, $\bar{V}_\Gamma$ the induced velocity due to the circulation distribution, and $\bar{V}_{\Gamma S1}$ and $\bar{V}_{\Gamma S2}$ the self-induced velocities on the upper and lower surfaces of the wing, respectively. The computer program devoted to this step is designed to execute one compressibility cycle and one wake cycle for each run due to the time limitation of NASA Langley's Cyber 175 computer.

Numerical Examples

Three ranges of subsonic Mach numbers and high angles of attack are considered in this paper.

For the nearly incompressible flow ($M_\infty \approx 0.0$), the inhomogeneous term of Eq. (5) is set equal to zero and the problem is solved using the wake iteration cycle only, which sequentially enforces the wing and the free vortex lines boundary conditions. Figure 2 depicts a typical converged solution after six-wake iteration cycles. The computed leading- and trailing-edge vortex cores (LEC, TEC) are also shown in the figure. On the wing surface a 10×10 vortex lattice has been used and the free wake computation has been carried up to one-chord length behind the trailing edge. The CPU time for this case is about 4 min on the Cyber 175.

For the second range of Mach numbers ($0<M_\infty<0.5$), the inhomogeneous term of Eq. (5) is retained as linearized compressibility [Eq. (10)] and the problem is solved in the equivalent incompressible space (Prandtl-Glauert transformation) according to Eqs. (12) and (13). The resulting equivalent incompressible flow problem is solved using the wake iteration cycles only. Figures 3 and 4 show the results of the total normal force C_n and pitching moment C_{mz} coefficients vs the angle of attack for two delta wings of aspect ratios 1 and 2, respectively. Wide ranges of subsonic Mach numbers are considered ($M_\infty = 0.0$-0.8 and 0.0-0.85). The results are compared with the experimental data of Refs. 32-34. In general, it is seen that for Mach numbers above 0.5 and for angles of attack above 8 deg, the computed results show deviation from the experimental data. This deviation becomes considerable for higher Mach numbers and higher angles of attack. This is attributed to the linearization of the compressible terms. It is clearly seen that the linear compressibility overpredicts the total load coefficients. This case converges after the same number of wake iteration cycles as that of the incompressible case, but it takes slightly more CPU time.

For the third range of Mach numbers ($0.5>M_\infty\leq0.7$, shock-free flows), the inhomogeneous term of Eq. (5) is given by Eq. (6) along with Eq. (4) with the exception of the first compressibility iteration cycle, which is based on the linear term given by Eq. (10). For the compressibility cycles, a three-dimensional grid (each elemental volume has a constant source strength) is constructed consisting of $17\times13\times13$ grid points in the x, y, and z directions, respectively. The step sizes are $\Delta x = 1.0$, $\Delta y = 0.25$, and $\Delta z = 0.25$. This grid size requires 2304 G calculations. Figures 5 and 6 show Mach number contours and leading-edge vortex shapes in cross-flow planes for a delta wing of aspect ratio of 1 at a 20.5 deg angle of attack and two freestream Mach numbers of 0.5 and 0.7, respectively. In

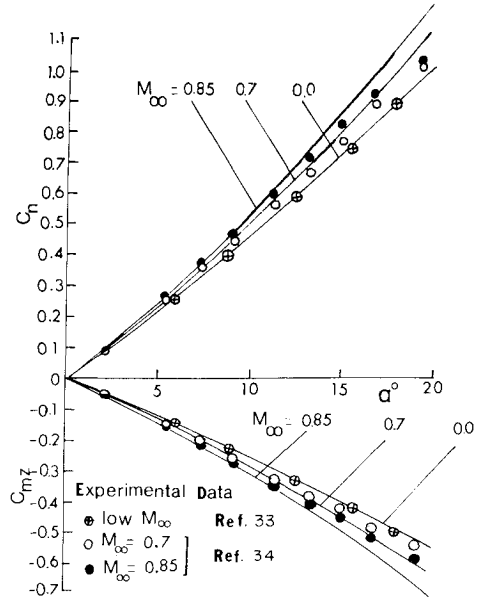

Fig. 4 Normal force and pitching moment coefficients vs angle of attack at different Mach numbers ($\mathcal{R}=2.0$, $G_i = M_\infty u_{xi}$).

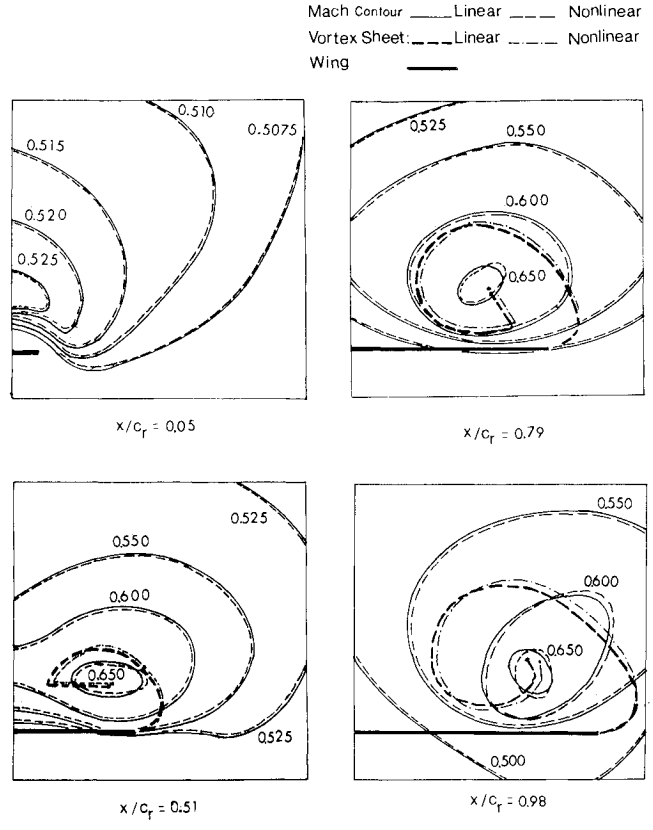

Fig. 5 Mach number contours and leading-edge vortex roll-up in cross-flow planes for a delta wing with linear and nonlinear compressibility effects ($M_\infty = 0.5$, $\alpha = 20.5$ deg, $\mathcal{R}=1$).

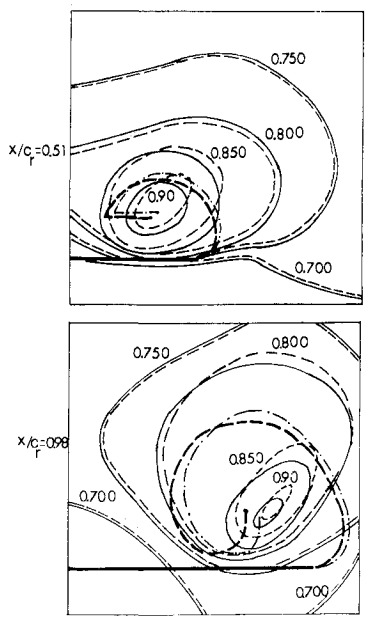

Fig. 6 Mach number contours and leading-edge vortex roll-up in cross-flow planes for a delta wing with linear and nonlinear compressibility effects ($M_\infty = 0.7$, $\alpha = 20.5$ deg, $\mathcal{R} = 1$).

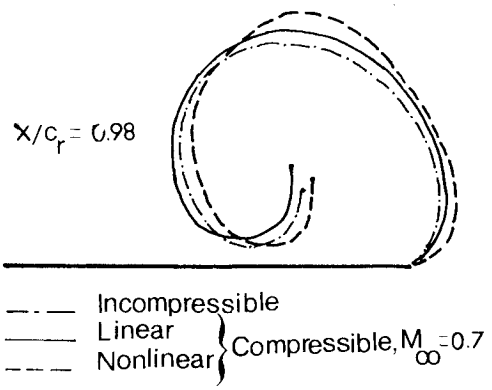

Fig. 7 Comparison of the computed leading-edge vortex roll-ups for incompressible and compressible flows past a delta wing ($M_\infty = 0.7$, $\alpha = 20.5$ deg, $\mathcal{R} = 1$).

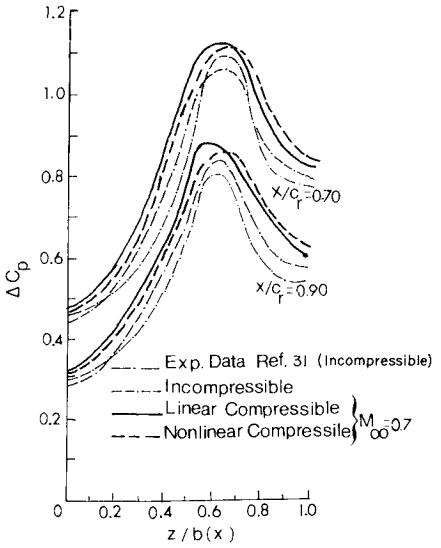

Fig. 8 Comparison of the spanwise net pressure variation for a delta wing ($M_\infty = 0.7$, $\alpha = 20.5$ deg, $\mathcal{R} = 1$).

these figures, we compare the results of the linear compressibility (Prandtl-Glauert transformation) with those of the nonlinear compressibility. For $M_\infty = 0.5$, one does not see appreciable differences in the forward cross-flow planes. Only in the trailing-edge region near the vortex core can one notice some differences.

For $M_\infty = 0.7$, one can clearly see appreciable differences in the shape and location of the Mach contours and the vortex sheets with the nonlinear compressibility as they move further outboard and upward. It is interesting to notice the closed near-sonic Mach contour at the vortex core, which indicates that a supersonic region might develop if one increases the freestream Mach number or the wing angle of attack.

Figure 7 compares the shapes of the leading-edge vortex sheet near the trailing edge for the incompressible flow and the linear and nonlinear compressibilities at $M_\infty = 0.7$. The results of the nonlinear compressibility show that the vortex core is nearer to the wing surface than that predicted with the linear compressibility or the incompressible flow.

Figure 8 compares the spanwise variation of the net pressure coefficient at two chord stations for the incompressible flow and the linear and nonlinear compressibilities at $M_\infty = 0.7$. The experimental data shown are for incompressible flow. It is evident that the linear compressibility overpredicts the loading. These results qualitatively agree with the experimental results of Vorropoulos and Wendt,[35,36] who experimentally tested a delta wing of aspect ratio of 2.

This case takes 10 wake iteration cycles and 4 compressibility iteration cycles until convergence is achieved. The CPU time is about 60 min on the Cyber 175. It should be noted that no effort has been made yet to write an efficient computer program for this problem.

Conclusions

A computational technique based on the integral solution of the full potential equation has been developed to solve the three-dimensional compressible flows past wings at large angles of attack. The full nonlinear compressibility terms are represented by a volume integral term approximated by a source distribution inside a finite volume around the wing.

The problem is solved by using double iteration cycles: wake and compressibility. The present technique does not increase the size of the influence coefficient matrix and hence no substantial increase is required in the core memory. Moreover, the required computational time is still reasonable when we recall the complexity of the problem under consideration. The initial computational results are very promising.

Although the present paper is limited to subcritical flows only, transonic flows at large angles of attack can be solved by using a shock-fitting technique that is under development.

Appendix: Velocity Induced by a Source Volume

The velocity potential at the field point $_p(x,y,z)$ due to a source volume of strength $G(\xi,\eta,\zeta)$ is given by

$$\phi_p(x,y,z) = \frac{1}{4\pi}\int_{\eta_1}^{\eta_2}\int_{\zeta_1}^{\zeta_2}\int_{\xi_1}^{\xi_2}\frac{G(\xi,\eta,\zeta)}{(A^2+B^2+C^2)^{1/2}}\,d\xi\,d\zeta\,d\eta \tag{A1}$$

where $A = x-\xi$, $B = y-\eta$, and $C = z-\zeta$.

Taking the gradient of Eq. (A1), the velocity is given by

$$\bar{V}_p(x,y,z) = -\frac{1}{4\pi}\int_{\eta_1}^{\eta_2}\int_{\zeta_1}^{\zeta_2}\int_{\xi_1}^{\xi_2}\frac{G(\xi,\eta,\zeta)(A\bar{i}+B\bar{j}+C\bar{k})}{(A^2+B^2+C^2)^{3/2}}\,d\xi\,d\zeta\,d\eta \tag{A2}$$

For constant G, the closed-form expression of the velocity is found to be

$$\bar{V}_p = \frac{G}{4\pi}\left[\eta \ln\left(\frac{HPC}{D}\right) - C \ln\left(\frac{HPB}{E}\right) - \frac{y}{2}\times\ln\left(\frac{HPC}{HMC}\right) - A\tan^{-1}\left(-\frac{BC}{AH}\right)\right]\bar{i} + \frac{G}{4\pi}\left[\zeta \ln\left(\frac{HPA}{F}\right) - A \ln\left(\frac{HPC}{D}\right) - \frac{z}{2}\right.$$
$$\left.\times\ln\left(\frac{HPA}{HMA}\right) - B\tan^{-1}\left(-\frac{AC}{BH}\right)\right]\bar{j} + \frac{G}{4\pi}\left[\xi \ln\left(\frac{HPB}{E}\right) - B \ln\left(\frac{HPA}{F}\right) - \frac{x}{2}\times\ln\left(\frac{HPB}{HMB}\right) - C\tan^{-1}\left(-\frac{AB}{CH}\right)\right]\bar{k} \tag{A3}$$

where

$$D=(A^2+B^2)^{1/2},\quad E=(A^2+C^2)^{1/2},\quad F=(B^2+C^2)^{1/2}$$
$$H=(A^2+B^2+C^2)^{1/2} \tag{A4}$$

$$HPC=H+C,\ HPA=H+A,\ HPB=H+B$$
$$HMC=H-C,\ HMA=H-A,\ HMB=H-B \tag{A5}$$

Acknowledgment

This work has been supported by NASA Langley Research Center, Hampton, VA, under Grant NSG 1560; Dr. E. Carson Yates Jr. is the technical monitor.

References

[1]Rehbach, C., "Calculation of Flow around Zero-Thickness Wings with Evolute Vortex Sheets," NASA TT F-15, 183, 1973.

[2]Kandil, O. A., Mook, D. T., and Nayfeh, A. H., "Nonlinear Prediction of the Aerodynamic Loads on Lifting Surfaces," *Journal of Aircraft*, Vol. 13, Jan. 1976, pp. 22-28.

[3]Kandil, O. A., Mook, D. T., and Nayfeh, A. H., "A Numerical Technique for Computing Subsonic Flow Past Three-Dimensional Canard-Wing Configurations with Edge Separations," AIAA Paper 77-1, Jan. 1977.

[4]Kandil, O. A., Atta, E. H., and Nayfeh, A. H., "Three-Dimensional Steady and Unsteady Asymmetric Flow Past Wings of Arbitrary Planforms," Unsteady Aerodynamics, AGARD CP-227, Feb. 1978, pp. 2.1-2.19.

[5]Kandil, O. A., "Numerical Prediction of Vortex Cores from the Leading and Trailing Edges of Delta Wings," ICAS Paper 14.2 presented at 12th ICAS Congress, Munich, FRG, Oct. 1980.

[6]Kandil, O. A. and Balakrishnan, L., "Recent Improvements in the Predictions of the Leading- and Trailing-Edge Vortex Cores of Delta Wings," AIAA Paper 81-1263, June 1981.

[7]Johnson, F. T. and Rubbert, P. E., "Advanced Panel-Type Influence Coefficient Method Applied to Subsonic Flows," AIAA Paper 75-50, 1975.

[8]Summa, J. M., "A Numerical Method for the Exact Calculation of Airloads Associated with Impulsively Started Wings," AIAA Paper 77-2, 1977.

[9]Johnson, F. T., Tinoco, E. N., Lu, P., and Epton, M. A., "Recent Advances in the Solution of Three-Dimensional Flows over Wings with Leading Edge Vortex Separation," AIAA Paper 79-0282, Jan. 1979.

[10]Hoeijmakers, H. W. M. and Vaatstra, W., "A Higher-Order Panel Method Applied to Vortex Sheet Roll-Up," AIAA Paper 82-0096, Jan. 1982.

[11]Luckring, J. M., Schoonover, W. E. Jr., and Frank, N. T., "Recent Advances in Applying Free Vortex Sheet Theory for the Estimation of Vortex Flow Aerodynamics," AIAA Paper 82-0095, Jan. 1982.

[12]Lamar, J. E. and Campbell, J. F., "Recent Studies at NASA-Langley of Vortical Flows Interacting with Neighboring Surfaces," Aerodynamics of Vortical Type Flows in Three-Dimensions, AGARD CP 342, April 1983, pp. 10.1-10.32.

[13]Chu, L., "Nonlinear Hybrid-Vortex Method for Wings Having Side-Edge Separations," M.S. Thesis, Old Dominion Univ., Norfolk, VA, Dec. 1980.

[14]Kandil, O. A., Chu, L., and Tureaud, T., "A Nonlinear Hybrid Vortex Method for Wings at Large Angle of Attack," *AIAA Journal*, Vol. 22, March 1984, pp. 329-336.

[15]Kandil, O. A., "Steady and Unsteady Incompressible Free-Wake Analysis," Lecture presented at the International School of Applied Aerodynamics, Amalfi, Italy, May 29-June 5, 1982.

[16]Suciu, E. O. and Morino, L., "Nonlinear Steady Incompressible Lifting Surface Analysis with Wake Roll-up," *AIAA Journal*, Vol. 15, Jan. 1977, pp. 54-58.

[17]Tseng, K. and Morino, L., "Nonlinear Green's Function Method for Unsteady Transonic Flows," *AIAA Progress in Astronautics and Aeronautics: Transonic Aerodynamics*, Vol. 81, edited by David Nixon, AIAA, New York, 1982, pp. 565-603.

[18]Ballhaus, W. F., "Some Recent Progress in Transonic Flow Computations," *Numerical Methods in Fluid Dynamics*, edited by H. J. Wirtz and J. J. Smolderen, Hemisphere Publishing Corp., New York, 1978, pp. 155-234.

[19]Schmidt, W., "Progress in Transonic Flow Computation," *Numerical Methods in Fluid Dynamics*, Hemisphere Publishing Corp., New York, 1978, pp. 299-338.

[20]Holst, T. L., "A Fast, Conservation Algorithm for Solving the Transonic Full-Potential Equations," *Proceedings of AIAA 5th Computational Fluid Dynamics Conference*, July 1979, pp. 136-148.

[21]Jameson, A. and Caughey, D. A., "Progress in Finite-Volume Calculations for Wing Fuselage Combination," *AIAA Journal*, Vol. 18, Nov. 1980, pp. 1281-1288.

[22]Grossman, B. and Siclari, M. J., "The Non-Linear Supersonic Potential Flow Over Delta Wings," AIAA Paper 80-0269, Jan. 1980.

[23]Siclari, M. J., "Computation of Nonlinear Supersonic Potential Flow Over Three-Dimensional Surfaces," AIAA Paper 82-0167, Jan. 1982.

[24]Minailos, A. N., "Calculation of Supersonic Flow Past Wings with Consideration of Tangential Discontinuities Shed from the Edges within the Scope of a Model Using a System of Euler Equations," *Fluid Dynamics*, Vol. 13, No. 1, Jan.-Feb. 1978, pp. 78-89.

[25]Klopfer, G. H. and Nielsen, J. N., "Euler Solutions for Wing and Wing-Body Combination at Supersonic Speeds with Leading-Edge Separation," AIAA Paper 80-0126, Jan. 1980.

[26]Marconi, F., "The Spiral Singularity in the Supersonic Inviscid Flow Over a Cone," AIAA Paper 83-1665, July 1983.

[27]Rizzi, A., "Damped Euler-Equation Method to Compute Transonic Flow around Wing-Body Combinations," *AIAA Journal*, Vol. 20, Oct. 1982, pp. 1321-1328.

[28]Krause, E., Shi, X. G., and Hartwich, P. M., "Computation of Leading Edge Vortices," *Proceedings of AIAA 6th Computational Fluid Dynamics Conference*, July 1983, pp. 154-162.

[29]*Rizzi, A., "Mesh Influence on Vortex Shedding in Inviscid Flow Computations," Recent Contributions to Fluid Mechanics*, edited by W. Haase, Springer Verlag, New York, 1982, pp. 213-221.

[30]Kandil, O. A., Mook, D. T., and Nayfeh, A. H., "Subsonic Loads on Wings Having Sharp Leading-Edges and Tips," *Journal of Aircraft*, Vol. 13, Jan. 1976, pp. 62-63.

[31]Hummel, D., "On Vertex Formation over a Slender Wing at Large Angles of Incidence," High Angle-of-Attack Aerodynamics, AGARD CP-247, Jan. 1979, pp. 15.1-15.17.

[32]Bateman, T. E. B. and Haines, A. B., "A Comparison of Results in the A.R.A. Transonic Tunnel on a Small and a Large Model of a Slender Wing," BARC, R&M 3287, 1961.

[33]Bartlett, G. E. and Vidal, R. J., "Experimental Investigation of Influence of Edge Shape on the Aerodynamic Characteristics of Low-Aspect-Ratio Wings at Low Speeds," *Journal of the Aeronautical Sciences*, Vol. 22, No. 8, 1955, pp. 517-533.

[34]Emerson, H. F., "Wind-Tunnel Investigation of the Effect of Clipping the Tips of Triangular Wings of Different Thickness, Camber, and Aspect Ratio—Transonic Bump Method," NACA TN 3671, 1956.

[35]Vorropoulos, G. and Wendt, J. F., "Preliminary Results of LDV Survey in the Compressible Leading Edge Vortex of a Delta Wing," VKI Tech. Note 137, Aug. 1982.

[36]Vorropoulos, G. and Wendt, J. F., "Laser Velocimetry Study of Compressible Effects on the Flow Field of a Delta Wing," Aerodynamics of Vortical Type Flows in Three Dimensions, AGARD CP 342, April 1983, pp. 9.1-9.13.